JOURNAL OF GEOPHYSICAL RESEARCH, VOL. 102, NO. A9, PAGES 19,845-19,859, SEPTEMBER 1, 1997

A study of the CDAW 9C substorm of May 3, 1986, using magnetogram inversion technique 2, and a substorm scenario with two active phases

V. M. Mishin,[1] L. P. Block,[2] A. D. Bazarzhapov,[1] T. I. Saifudinova,[1]
S. B. Lunyushkin,[1] D. Sh. Shirapov,[1,3] J. Woch,[4,5], L. Eliasson,[4]
G. T. Marklund.[2] L. G. Blomberg,[2] and H. Opgenoorth[6]

Abstract. One of the CDAW 9C substorms is investigated in this paper using the database reported by Hones et al. and supplemented with magnetogram inversion technique (MIT) 2 data. These latter have provided information about the dynamics of the open tail magnetic flux, current systems in the ionosphere, and the size and dynamics of the current wedge. We have identified the growth, expansion, and recovery phases of this substorm, with characteristics expected from a generally accepted scenario. However, specific signatures were observed in the interval (0919-0935) UT, i.e., between the growth and expansion phases, indicating the concurrent development of the substorm onset and corresponding instabilities in the innermost current sheet, and small-scale cross-tail current disruptions without the open tail reconnection. In addition to signatures of small-scale dipolarization, an increase of the open tail magnetic flux, and a current system of the type close to *DP* 2 were observed at (0919-0935) UT, which is more likely to suggest predominance of the tail-stretching process than magnetic collapse. This fact was interpreted in terms of a relevant simple model as a signature of the growth of the energy input from the solar wind which ensures the observable disturbance power. Hence the disturbance at (0919-0935) UT was more likely a driven one than an unloading one. The aforementioned signatures make it possible to identify the interval (0919-0935) UT as the "phase of multiple onsets" or (equivalently) the "first active phase," which was previously defined by *Mishin* [1991, and references therein] as one of the four standard phases of a typical substorm (in addition to the expansion phase). Thus the case study supports the substorm scenario with two active phases and, accordingly, with two different kinds of physics. This case study illustrates also the informativity of MIT 2 data and their ability to effectively complement the database traditionally used in substorm studies.

1. Introduction

The term "magnetospheric substorm" was coined by *Akasofu* [1968] and *Coroniti et al.* [1968]. The subsequent 30 years saw the emergence of a number of substorm models, which, however, differ even conceptually.

From observations it follows that there exist two main types of large-scale processes that initiate a typical substorm: processes of tail magnetic energy storage (growth phase by *McPherron* [1970]) and processes of explosive release of accumulated energy (substorm onsets). There is little doubt that the second type of processes are caused by tail current disruptions. However, these disruptions can be localized in the closed part of the tail, or they can also encompass the open tail. In the latter case a large-scale, near-Earth neutral line (NL) is produced. In the popular substorm model [e.g., *Baker et al.*, 1994] it is this process of NL formation that sets up the substorm active phase (expansion phase).

The alternative RBSF, Kan, and Lui models were constructed by *Rothwell et al.* [1988a, b, 1989, 1991], by *Kan* [1993, and references therein], and by *Lui* [1991, and references therein], respectively. In these models, the tail current disruption is caused by nonlinear magnetosphere-ionosphere coupling. Plasma sheet reconnection is a secondary effect of current disruption.

[1]Institute of Solar-Terrestrial Physics, Russian Academy of Sciences, Irkutsk, Russia.

[2]Alfven Laboratory, Department of Plasma Physics, Royal Institute of Technology, Stockholm, Sweden.

[3]Now at East Siberian State Technology University, Ulan-Ude, Russia

[4]Swedish Institute of Space Physics, Kiruna, Sweden.

[5]Now at Max-Planck-Institut für Aeronomie, Katlenburg-Lindau, Germany

[6]Swedish Institute of Space Physics, Uppsala, Sweden.

Paper number 97JA00154.
0148-0227/97/97JA-00154$09.00

In the K model the expansion phase is driven by the solar wind dynamo, and substorms can occur without a near-Earth neutral line. In a new substorm model by *Lyons* [1995, 1996], the substorm expansion phase is also treated as a driven (i.e., not spontaneous) process, but the driving factor is a decrease of the solar wind electric field **E**. In order for the expansion onset to be "turned on," it is necessary, according to this model, to turn off or attenuate the solar wind - magnetosphere dynamo. No other types of substorm onsets (spontaneous substorm onsets) exist in this model.

The present paper is concerned with an attempt to study different kinds of substorm onsets and their relation to the formation of a near-Earth NL. With this object in view, we make use of the magnetogram inversion technique (MIT) 2 for determining the polar cap boundary, making it possible to calculate its area S and the magnetic flux in the open tail, $\Psi = SB$, where B is a mean value of the geomagnetic field strength in the polar cap. Plots which show the variation of Ψ in the course of substorms, obtained by MIT 2 at time steps of about 1-10 min, are the aforementioned principal additional information.

These plots of Ψ values were obtained by Mishin et al. for more than 30 substorms investigated by these authors, including 10 events that were also studied by other workers within the CDAW 6 and CDAW 9 projects [see *Mishin et al.*, 1992a; *Mishin*, 1991; and references therein]. In all of the aforementioned cases without exception, it was found that the open magnetic flux Ψ increases in the course of the first two substorm phases, thus signalling the magnetic energy storage in the tail up to about $10^{21} - 10^{22}$ erg. This process is interrupted spontaneously, or because of a northward turning of the interplanetary magnetic field (IMF), and gives way to form a near-Earth neutral line and a rapid decrease of Ψ, the beginning of which coincides with expansion onset. During the subsequent expansion phase the earlier accumulated energy of the order of $10^{21} - 10^{22}$ erg is dissipated.

Thus the results obtained lend support to the model with a near-Earth NL. These results also favor the conclusion that the expansion phase is not controlled directly by the solar wind, but to a greater extent it has an unloading character [cf. *Baker*, 1992; *Akasofu*, 1992].

Moreover, additional information leads us to conclude that in a typical substorm there exists, apart from the known growth, expansion, and recovery phases, one more phase, which differs from the aforementioned ones in that it involves plasma sheet instabilities and corresponding substorm onsets, but in the innermost plasma sheet only and without the formation of a large-scale near-Earth neutral line. This phase, observed after growth and prior to expansion, was called the "first active phase" or the "phase of multiple onsets." The observed disturbance power in this phase is usually less than but comparable with that of an expansion phase, although the main energy source is provided by the solar wind; i.e., this phase is largely a driven rather than unloading one. The results obtained do not support supposition that the development of the substorm active phase is controlled by the tailward propagation of an impulse of decrease of the electric field $\mathbf{E}_{SW}$, because multiple onsets of the first active phase appear spontaneously.

New information due to MIT 2 (plots of Ψ and other parameters calculated based on Ψ) led also to the conclusion that the sequence of the first three phases of a typical substorm (i.e., the sequence of growth, multiple onsets, and expansion phases) is organized through a common global process that was called the "tail stretching feedback" (TSF for short). TSF provides development of growth phase and multiple substorm intensifications without large-scale neutral line formation and prepares the explosive transition to the expansion phase created by the open tail reconnection [*Mishin et al.*, 1992a; *Mishin*, 1991, and references therein].

Taking into consideration some methodological features and the fact that they (and MIT 2 as the whole) are not well known to the Journal of Geophysical Research (JGR) readership, the present paper includes a more detailed outline of these features. Thus this work is a first (written for JGR) paper concerned with the aforementioned MIT 2 methods of determining Ψ and parameters derived from Ψ, as well as with the application of these methods for timing and investigating the CDAW 9C substorm. Section 2 gives an outline of MIT 2. In this section we also describe procedures for calculating (on the basis of Ψ) some other parameters. Subsequent sections describe a selected example substorm with allowance made for additional information which is used in conjunction with a traditional set of observations.

2. The MIT 2 Method

The magnetogram inversion technique (MIT) is a method to calculate a two dimensional (2-D) spatial distribution of both the ionospheric electric field and currents. It uses as inputs (1) measurements from a large number of ground-based magnetometers and (2) a carefully selected model of the ionospheric height-integrated conductivity tensor $\hat{\Sigma}$. MIT was used by *Mishin* [1968] and *Mishin et al.* [1979, and references therein]. The well-known KRM technique [*Kamide et al.*, 1981] is one variant of the MIT. A generalization of this method allows use of satellite electric and magnetic field measurements as additional inputs [*Richmond and Kamide*, 1988]. Input of auroral imager data provides more realistic instantaneous conductivity models [*Marklund et al.*, 1987]. For a review, see *Mishin* [1990]. Having a global system of ionospheric currents obtained from ground-based magnetometers, and a realistic model of the spatial distribution of $\hat{\Sigma}$ one may calculate a series of other standard MIT outputs, including the ionospheric Joule heating and the distribution of field-aligned current (FAC) density.

Major advantages of MIT methods compared with other methods are that: (1) outputs may be calculated with high time resolution ($\Delta t = 1$ min or under special conditions $\Delta t = 10$ s), and (2) it gives a global instantaneous survey of the ionospheric electric field **E** and currents.

A major disadvantage is poor spatial resolution: 300-500 km or ~200 km for a locally denser magnetometer chain With this spatial resolution, the typical errors in **E** are < 10-20% for latitudes higher than ~60°. More importantly, however, these errors are strongly dependent on the conductivity model (see the reviews by *Mishin* [1990] and *Richmond and Kamide* [1988]).

However, the main conclusions reported in this paper were drawn on the basis of MIT 2 data, i.e., on the basis of the part of the MIT data that is virtually independent of the ionospheric conductivity model.

MIT 2 is an extension of MIT which enables calculation of some other, physically very interesting parameters derived from the polar cap (PC) boundary as determined from the FAC distribution, assuming the PC boundary coincides with the high-latitudinal boundary of FAC region 1 (for an example, see Figure 3 and its description in the text). Thus MIT 2 errors are determined by those resulting from determining the aforementioned boundary using FAC density distributions. As has been pointed out, FAC density values depend on the conductivity model used. However, many years of experience of MIT work show that the position of the FAC region 1 boundary does virtually not change in going (in MIT calculations) from one conductivity model to another reasonably chosen model. In practice, therefore, it is even possible to use a spatially homogeneous conductivity model (when determining the polar cap boundary). The location of PC boundaries in this case coincides with that for inhomogeneous conductivity within 1°- 3°of latitude; PC areas for the aforementioned conductivity models coincide within ±10%. Thus irrespective of the ionospheric conductivity model used, errors of determining the polar cap area turn out to be rather small; they lie within those of the more direct methods. The main reason for the relatively small errors of MIT 2 is, perhaps, that the most significant FACs appear near or at the electrojets, which give the most clear signatures on the ground Thus quantitative errors in FAC density may be large, but errors in FAC locations are small.

Mishin et al. [1992a] compared results of the MIT 2 method of determining the polar cap boundary both with statistical results of an independent method by *Elphinstone et al.* [1991], who used Viking auroral images, and with the result by *Birn et al.* [1991], who used the Tsyganenko-1987 model. In both cases the deviation of the PC boundaries obtained by the two methods did not exceed 1°–3°of latitude. The third comparison with DE 1 data [*Baker et al.*, 1994] gave the worst (though satisfactory) result, shown in Figure 1. Here the variations of the magnetic flux through the polar cap area S are shown in a course of the substorm of 0000-0300 UT, May 3, 1986, obtained by two methods. The plot of Ψ_{DE} was obtained using auroral images. The values of Ψ_{MIT} calculated by MIT 2 [*Mishin et al.*, 1992b, Figure 1]. One can see that the greatest discrepancy of the results from two methods does not exceed 25%. Importantly, the maxima of Ψ on the two plots coincide in time. It is the time of a maximum Ψ that is used as expansion onset when timing the substorm.

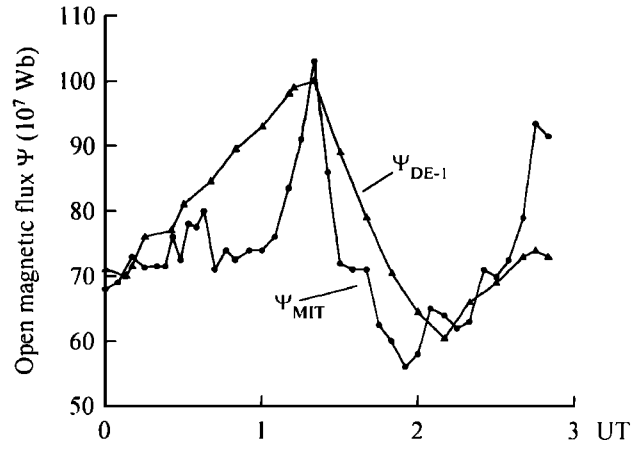

Figure 1. Variations of the magnetic flux through the polar cap (Ψ) in the course of the substorm of May 3, 1986, 0000-0300 UT. Ψ_{DE} is Ψ from DE 1 data *Baker et al.* [1994]; Ψ_{MIT} is from MIT 2 data.

The major parameters determined by MIT 2 are the following:

Polar cap magnetic flux. The polar cap magnetic flux is given by

$$\Psi = B_0 S \tag{1}$$

where B_0 is the average magnetic field in the polar cap and S is the polar cap area.

Polar cap flux Ψ_2. The polar cap flux Ψ_2 is a value of Ψ at the most quiet conditions when the Perreault-Akasofu index $\varepsilon \Rightarrow 0$. For more active periods we can then write

$$\Psi = \Psi_1 + \Psi_2 \tag{2}$$

where Ψ_2 corresponds to the reference level when the IMF $B_Z = B_Y = 0$, and Ψ_1 is the excess polar cap flux at higher activity.

The flux Ψ_2 is probably closed during quiet periods, although it may include some small open flux within it. The closed part must be due to "viscous drag" pulling the field lines to the far end of the tail, thus causing the minimum auroral and magnetic activity prevailing during even the most quiet periods. During higher activity, more flux Ψ_1 is added to the polar cap magnetic flux. The method of determining Ψ_2 is given below and, in more detail, by *Mishin* [1990, section 2]. Knowing Ψ and Ψ_2, we can then calculate Ψ_1 from (2).

Figure 2 gives a typical example of a Ψ plot for a time interval containing both quiet and substorm periods. One can see a significant value of Ψ (~4×10^8 Wb) even at the most quiet time (before 2045 UT) when the Perreault-Akasofu index $\varepsilon \Rightarrow 0$. The Ψ values are increased during substorms by a factor of 2-3, at most, as seen in Figure 2. Statistically, Ψ_2 depends on the solar wind kinetic energy flux $P_d = (nV^3)^{1/2}$ according to

$$\Psi_2 = 22 + 5P_d \tag{3}$$

in units of 10^7 Wb, $P_d(10^{12}\mathrm{s}^{-3/2}) = 3.2\times10^{-5}(nV^3)^{1/2}$, where n is in reciprocal centimeters cubed and V is

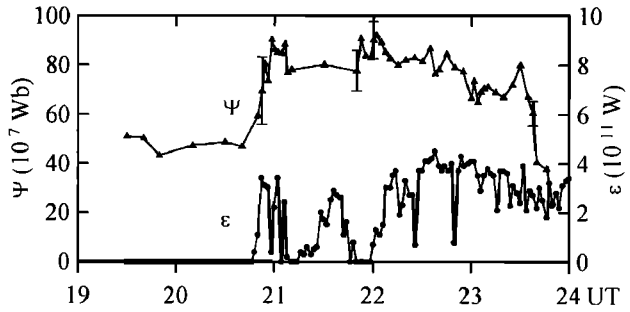

Figure 2. Illustration of the method to determine the polar cap flux Ψ_2 at quiet conditions when the Perreault-Akasofu index $\varepsilon \Rightarrow 0$. That is the case in the event shown before 2045 UT at September 25, 1986.

in kilometers per second. The regression equation (3) is obtained by the method of least squares. Sixteen pairs of Ψ_2 and P_d values are used for quiet intervals in March-May 1986.

There are thus two alternative ways of determining Ψ_2: by assuming it as the reference level of Ψ observed before an isolated substorm when ε is negligible, and from equation (3). Experience suggests that the differences between Ψ_2 values obtained by the two methods do not exceed 25%.

If the conclusions stated above are valid, two physically different parts of the polar cap flux exist, consistent with DMSP particle observations by *Akasofu et al.* [1992, p.1513]. They found that "there is an annular belt of precipitation of soft electrons (~300 eV) which extends poleward from the auroral oval." Inside this belt is the polar rain on open field lines. The size of this open region, "at least for both medium and weak substorms ... varies roughly in harmony with the AE index." Figure 4 of [*Akasofu*, 1992] shows that there exists also a near-pole part of the polar cap which does not disappear in the quietest periods of more than 24 hours, during which the AE index remained on a level below 100 nT.

We associate Ψ_1 and Ψ_2 with the variable part of the polar cap and with its near-pole part that remains at quiet times, respectively.

Poynting vector flux. The Poynting vector flux into the magnetosphere is the third major parameter to be found from MIT 2 analysis. It may be expressed as

$$\varepsilon' = \Psi_1^2 V/(\mu_0 S_T) \tag{4}$$

assuming that Ψ_1 alone represents open flux; $\mu_0 = 4\pi \times 10^{-7}$H/m; V is the solar wind speed; and S_T is the total cross section of the magnetotail lobes, containing all open flux. Indeed, formula (4) may be rewritten as

$$\varepsilon' = W_B S_T V \tag{5}$$

where W_B is the energy density of the magnetic field. Furthermore, let W_E be the energy density of the electric field in the plasma, and let C be the speed of light. It is known from electrodynamics that when

$$V^2 \ll C^2$$

then the inequality holds

$$W_B \gg W_E \tag{6}$$

As a result, we get expression (4) [*Piddington*, 1963, *Siscoe and Cummings*, 1969; *Akasofu*, 1977; *Hill*, 1983; *Mishin*, 1990]. At given Ψ and V, formula (4) may be regarded as a trivial corollary of the definition of ε' as the electromagnetic energy flux $(W_B + W_E)S_T V$ from the solar wind into the magnetosphere under the condition (6). In (4), ε' is in watts, V is assumed to be available from ISEE 3 or IMP 8 measurements, and $S_T = \pi R_T^2$, where R_T is the open magnetotail radius. We assumed that the appropriate value for substorms is $R_T = 22.5\ R_E$. In fact, R_T is a weakly variable quantity. At $|x| \sim (10-20)\ R_E$, R_T values increase during the substorm within $\sim (18-25)\ R_E$ [*Akasofu*, 1977, and references therein]. Therefore, assuming R_T=const, we somewhat overestimate the range of variation of ε'.

Efficiency of power generator and tail length. The efficiency κ of the power ε' generator and tail length l_T can be estimated in the framework of the 2-D Dungey model using the MIT parameter Ψ_1 and solar wind parameters measured by a satellite. For this purpose, we now consider the continuity equation for open magnetic flux Ψ_1 [*Russell*, 1979]

$$M - R = d\Psi_1/dt \tag{7}$$

Here M is the magnetic merging rate at the dayside neutral point N_1, and R is the reconnection rate at the nightside neutral point N_2.

According to *Kan and Lee* [1979],

$$M(kV) = \sqrt{(\mu_0/4\pi)\varepsilon V} \tag{8}$$

where

$$\varepsilon = (4\pi/\mu_0) V B^2 \sin^4(\theta/2) l_0^2 \tag{9}$$

Here ε is the well-known index by *Perreault and Akasofu* [1978].

Suppose

$$R(t) = M(t - \Delta t) \tag{10}$$

$$\Delta t = l_T/V \tag{11}$$

where t is time; and l_T is the tail length, i.e., the distance between N_1 and N_2. For $t > t_0 + \Delta t$ we then have

$$\Psi_1 = M l_T/V \tag{12}$$

if it is further assumed for the sake of simplicity that $M = 0$ when $t < t_0$ and M=const>0 when $t > t_0$. From (12) and (4) it follows that

$$\varepsilon' = M^2 l_T^2/\mu_0 V S_T \tag{13}$$

whence it is evident that when M=const the input power ε' varies as l_T^2. In other words, the efficiency κ of the power ε' generator is proportional to l_T^2, i.e.,

$$\kappa = (l_T/l_{T0})^2 \tag{14}$$

where l_{T0} is some basic (invariable) value. We next note that the quantities ε in (9) and ε' in (13) both have the same meaning. We may write $\varepsilon = \varepsilon'$ when $l_T = l_{T0}$. From (13) we then have

$$\varepsilon = M^2 l_{T0}^2 / \mu_0 V S_T \tag{15}$$

where M is defined by expression (8). From (13)-(15),

$$\kappa = \varepsilon'/\varepsilon \tag{16}$$

Hence values of κ can be estimated by two methods using either (14) or (16).

Location of western end of westward electrojet. Knowing the equivalent current system, the location (latitude, Φ_N, and MLT, t_W) of the western end of the westward electrojet can be found which coincides with the Harang discontinuity center in *DP* 2 but not *DP* 1. The parameters t_W and Φ_N (especially the former) can serve as indicators of the type of equivalent current system: the value of t_W ~23 hours of MLT corresponds to the *DP* 2 type, i.e., to a two-vortex current system existing under quiet conditions and at substorm before the appearance of the current wedge or, equivalently, before the appearance of cross-tail current disruption. The system of real ionospheric Hall currents is qualitatively identical to the equivalent current system. Therefore the dynamics of the latter qualitatively reflects also the dynamics of the convection system (i.e., $\mathbf{E} \times \mathbf{B}$ - drift) of ionospheric plasma: under quiet conditions this latter also has the *DP* 2 type.

Disruption of cross-tail current produces a current wedge which includes the ionospheric westward electrojet [e.g., *McPherron et al.*, 1973, and references therein]. The superposition of the latter on *DP* 2 currents enhances the preexisting westward auroral electrojet and weakens the eastward one. Thus the overall current system is altered: the morning vortex (containing the westward electrojet) is enhanced, and the eastward vortex is partially suppressed. The system becomes a quasi-one-vortex system, which is denoted by the symbol *DP* 1. For an example of the *DP* 2 ⇒ *DP* 1 transition described above, see Figure 3a. "Clean" *DP* 2 and "clean" *DP* 1 are observed at 0915 UT and 0940 UT, respectively. It is evident that the *DP* 2 ⇒ *DP* 1 transition is characterized by a variation of t_W from ~2300 MLT to 1500 MLT (magnetic local time) and by a variation of Φ_N from 67° to ~75°. Such variations of t_W are typical of substorms, although their swing varies within 4-8 hours of MLT. (For details, see *Mishin* [1991]). From the foregoing discussion it follows that the *DP* 2 ⇒ *DP* 1 transitions characterize the current wedge dynamics. As will be apparent in the following, plots of t_W and Φ_N are used as one of tools for timing substorms, i.e., to determine phase start times.

Power input - internal dissipation difference. For the same purpose (substorm timing) the difference between power input and internal dissipation

$$P = \varepsilon' - Q_T \tag{17}$$

may be used. (We use Q_T synonymously with U_T of *Akasofu* [1981] to avoid confusion with universal time, UT). The sign of P is a signature of driven ($P > 0$) or unloading ($P < 0$) substorm phases.

The total substorm dissipation power was calculated from

$$Q_T = 2Q_i + 2Q_A + Q_{DR} \tag{18}$$

Akasofu [1981] has described how to estimate Q_T. We estimate Q_T (in watts) from

$$Q_i = \int_S \Sigma_p E^2 dS \tag{19}$$

$$Q_A = 1.2 \times 10^8 AE \tag{20}$$

$$Q_{DR} = 4 \times 10^{13} (d\overline{D}_{st}/dt + \overline{D}_{st}/\tau) \tag{21}$$

The unit for $\overline{D}_{st}$ and AE is in nanoteslas. The bar above D means "corrected for solar wind pressure," S is the area limited by $\Phi = 60°$, and τ is the characteristic ring current decay time. The values of τ from 0.5 to 7 hours will be used in the present study of the CDAW 9C substorm, according to *Gonzalez et al.* [1989]. (see section 4 for details).

It was noted by *Zwickl et al.* [1987] that Q_T depends critically on the characteristic time τ, which is known with large uncertainty. However, due to the fast increase in Q_T at expansion phase onset, the timing obtained from the change of sign of P is not correspondingly uncertain. In our experience, the uncertainty in timing is a few minutes, and often less. Additional use of other methods of substorm timing (the methods described in section 4) can decrease the error significantly. Thus MIT provides a significant amount of additional information about substorm processes.

In the next sections we describe the event of May 3, 1986. The case considered below was not the most favorable because solar wind parameters were unavailable. However, the main goal is to ascertain either the absence or the presence in the substorm of two types of substorm onsets with or without large-scale current wedge and, correspondingly, with decreasing or increasing Ψ_1. An additional (to the plot of Ψ_1) and independent signature of the occurrence of large scale current wedge is provided by information on the *DP* 2 ⇒ *DP* 1 transition. Such data (for both Ψ_1 and *DP* current systems) are available for the present study, as are a wealth of other data which are traditionally used. An important advantage of the event under consideration is that this substorm has already been subjected to a preliminary study. This circumstance simplifies our study greatly.

3. The Event on May 3, 1986

The substorm at 09-11 UT on May 3, 1986, was studied by *Hones et al.* [1987, also E. W. Hones Jr. et al.,

An auroral surge associated with plasma sheet recovery and its implications regarding behaviour of the substorm neutral line: CDAW 9, unpublished manuscript, 1993] as part of the CDAW 9 campaign, since it provided a good example of auroral surge formation associated with plasma sheet recovery and tailward retreat of the substorm neutral line. Viking images over the northern polar cap and DMSP-F7 images over the southern polar cap were used, as were plasma and magnetic field data from ISEE 1 and 2 about $17R_E$ tailward of Earth and $3R_E$ duskward of the magnetotail axis. Data from the 1984-129 geosynchronous satellite and ground-based magnetometer data from the Alaska chain and from some Canadian and Russian stations were also used.

The ISEE 1 and 1984-129 satellites were close to the 2300 MLT meridian, and the Alaska chain was near 2200 MLT. In order to relate the tail magnetic field and plasma variations to the evolution of the aurora the Tsyganenko-1987 magnetic field model was employed using the technique of *Jankowska et al.* [1990] and *Elphinstone et al.* [1990, 1991].

The data clearly show that there were two substorm onsets, at 0919 UT and 0936 UT. However, the first one was limited (as seen by ground magnetometers) to a narrow sector of the auroral oval at the magnetic latitude range $\Phi = 60° - 65°$ and within the 2-hour interval 2100-2300 MLT. Magnetic disturbances and bright auroral forms were localized inside that small region until 0936 UT. Plasma sheet thinning was observed on ISEE 1 and 2, beginning within a few minutes around 0919 UT. ISEE 1 revealed that a rapid earthward flow of plasma began at about 0915 UT. The 1984-129 satellite registered electron injection (30-300 keV) near 0919 UT.

In a summary of these data, Hones et al. (unpublished manuscript, 1993) suggested that the substorm neutral line was formed at ~0919 UT, probably somewhat tailward of ISEE 1 ($-17R_E > x > -26R_E$). Note for later discussion, however, that the ISEE 1 magnetometer showed field line stretching during the 0830-0935 UT interval (Hones et al., unpublished manuscript, 1993, Figure 8). There was no dipolarization simultaneously or shortly after the particle injection at 0919 UT.

Important changes began near 0936 UT. ISEE 1 recorded the start of a radial dipolarization at about that time. The 1984-129 satellite measured a second 30 to 300 keV electron injection event. On the ground the magnetometers registered both a poleward ($> 4°$) and east-west widening of the disturbed region, as well as strongly enhanced activity level after 0936 UT. Viking images (R. Elphinstone, private communication, 1994) revealed a similar widening and brightening of the auroral spot. At 0923 UT a weak spot was located at Φ_m ~63°-71°and ~2040-2320 MLT; at 0936 UT a bright aurora was seen at Φ_m ~63°-71°and ~2100-0130 MLT.

The events up to 0951 UT have been summarized by Hones et al. (unpublished manuscript, 1993) as follows: "After about an hour of increasing stretching of the tail field, expansive phase onset began at 0919 or 0936 UT and plasma sheet thinning occurred. By 0950 UT the auroral expansion had ceased, leaving a thickened nightside oval extending over many hours of local time, and there is evidence that the substorm neutral line was placed at $x_{GSM} \leq 26R_E$." Earlier in the same paper, they described the events as follows: "By ~0951 UT the poleward expansion had faded ... This was the end of the expansive phase and the beginning of the recovery phase. ... At ~ 0951 UT a bright spot became evident on the poleward border between 22 and 23 MLT in a Viking image. This persists ... and assumes the shape of an auroral surge in several of the Viking images. These reveal that ... by 1017:45 UT the surge had moved about one hour of local time westward."

By approximately the same time (after 0954 UT) a plasma sheet recovery was observed by ISEE 1. Hones et al. (unpublished manuscript, 1993) suggested "that the envelopment of ISEE 1 by plasma resulted when a plasma sheet thickening wave moving duskward across the tail reached ISEE. This thickening wave was the projection of the surge seen in both hemispheres." They also observed an upward field-aligned current at the surge head with a density, at 1005-1007 UT, of ~2 $\mu A/m^2$ and total intensity of $\sim 4 \times 10^5 A$. Their main conclusion is that the FAC flowing upward in the head of the auroral surge mapped to the leading edge of a wave of plasma sheet thickening that was advancing duskward across the tail. They infer that the thickening wave was "a manifestation of segmental retreat of the substorm neutral line."

Note also that *Hones et al.* [1987, also unpublished manuscript, 1993] determined the substorm phases as follows: expansion phase from 0919 or 0936 until 0950 UT, and recovery phase from 0951 UT. Now let us look at the MIT 2 data.

4. MIT 2 Data Presentation

In the present work, 83 ground-based magnetic stations [*Mishin et al.*, 1992b, Appendix 1] and the ionospheric electric conductivity model of *Mishin et al.* [1986] were used as inputs for the MIT method described in section 2 above. The quiet day May 22, 1986, was chosen as reference level for the geomagnetic field variations. The MIT 2 outputs most important for this study are parameters Ψ_1, ε', t_W, and Φ_N.

The method of determining Ψ, conformably to the event concerned, is illustrated in Figure 3b and is described in the text devoted to the analysis of this figure. Calculating $\Psi_1 = \Psi - \Psi_2$, the value of $\Psi_2 = 28 \times 10^7$ Wb has been used, corresponding to the minimum Ψ-value observed in the interval upon consideration (i.e., May 3, 0000-1030 UT). For calculating ε' using (4), it was necessary to have the values of the solar wind velocity V, which were unavailable in the interval 0919-1030 UT. Therefore we used V=500 km/s as the expected characteristic value for substorm. This assumption can affect the absolute values of ε' but not the essential

conclusions in the present paper with regard to substorm timing. For the latter, the moments in time where the difference $\varepsilon' - Q_T = 0$ were used as an additional signature. This difference depends on the value of V. However, it was found out that these moments in time do not change (within a few minutes) in the interval $V = (500 \pm 100)$ km/s. Nevertheless, the plot of differences $(\varepsilon' - Q_T)$ will be used in the present paper only to be sure that the plot does not contradict the conclusions inferred independently.

Figure 3 shows the evolution of the equivalent ionospheric current and FAC system during the substorm.

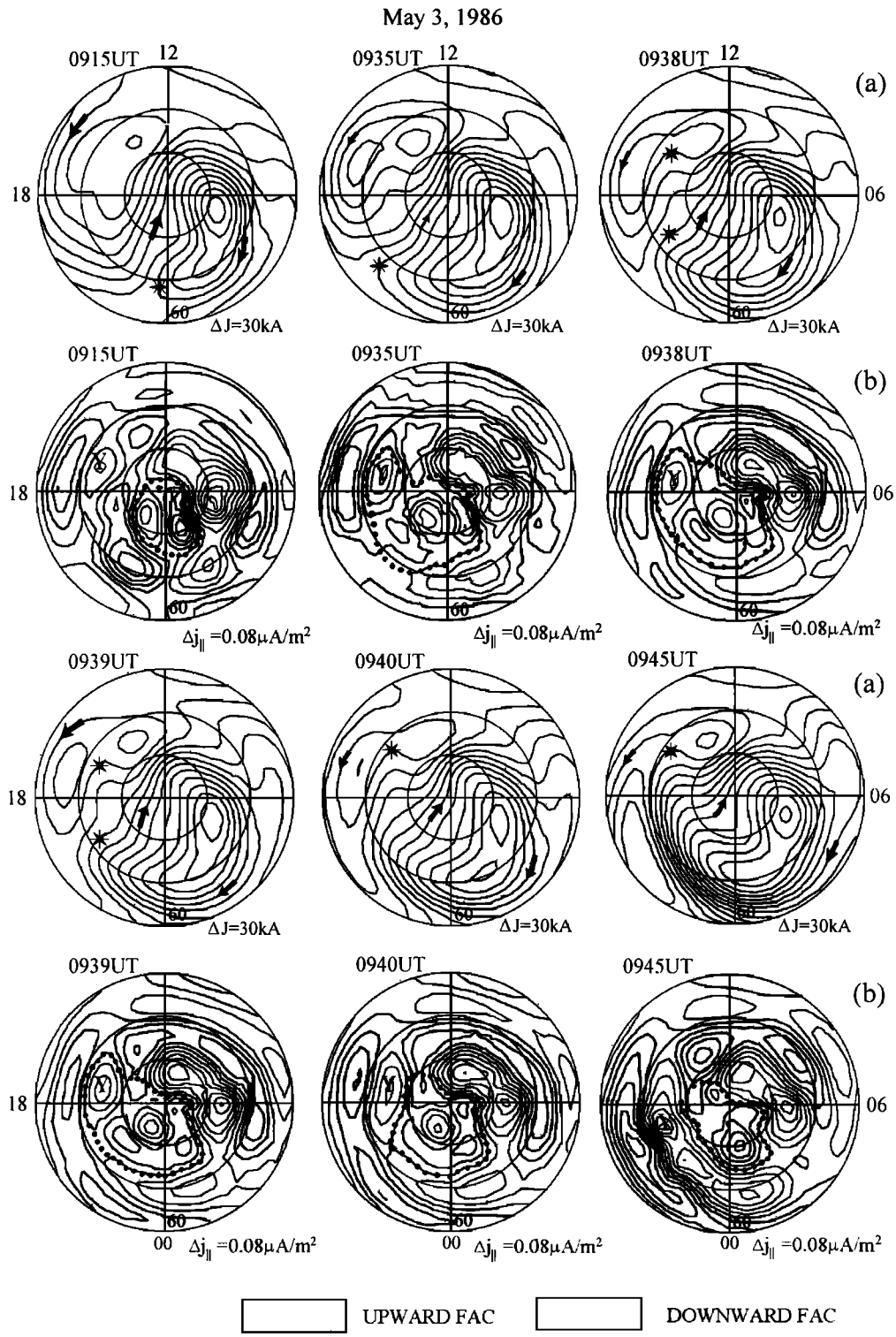

Figure 3. (a) MIT equivalent current systems and (b) MIT FAC density distributions for the CDAW 9C substorm. The dotted contours in Figure 3b are the polar cap boundaries. Asterisks in Figure 3a indicate the western end of the westward electrojet. A strong N-W twisting (expansion) of the electrojet is seen. The downward FAC region 1 extends through the morning and evening sectors at 0940 and 0945 UT. See text for greater details.

Five moments were chosen: 0915 UT before the first substorm onset, 0935 UT just before the second onset, and 0938, 0939, and 0940 UT during the final (global) stage of the second substorm onset.

The western termination of the westward electrojet is shown as an asterisk in Figure 3a. That is the point where the zonal component of the electrojet changes its sign. When this termination is located around midnight, the current system is of *DP* 2 type, i.e., it does not contain current wedge and corresponds to a classical two-vortex system of ionospheric plasma convection. A displacement of the discontinuity to the evening sector means a northwestward expansion of the westward auroral electrojet and, simultaneously, indicates the *DP* 2 ⇒ *DP* 1 transition. The reason for the transition is the superposition of a large-scale current wedge on *DP* 2-currents (see section 2).

From Figure 3a it is evident that at 0915 UT a clear *DP* 2 type is observed; at 0935 UT one can observe the initial stage of the *DP* 2 ⇒ *DP* 1 transition. The signature is a weak decrease of t_W (see also Figure 4). The similar type of the current system (i.e., *DP* 2 rather than *DP* 1) was observed until 0938 UT, when an acceleration of the global process was began. The two asterisks shown in Figure 3a at 0938 and 0939 UT, mark the terminations of two westward electrojets which were clearly separated in *DP* 2 type, but they merge together upon completion of the transition to *DP* 1 type. (One of these jets, at higher latitudes, is closure current of the eastward auroral electrojet in the evening sector.) Time 0938-0939 UT corresponds to the prefinal stage of merging of the two westward electrojets. At 0940 UT this merging is observed in Figure 3a as the completed event; i.e., a clear *DP* 1 type is observed. Only one auroral electrojet exists at this time, and it continues all the way to ~1600 MLT, while the eastward auroral electrojet is suppressed. A similar type, i.e., a clear *DP* 1, was observed long time after 0940 UT. The same pattern of *DP* 2 ⇒ *DP* 1 evolution is observed in Figure 4 , showing plots of the geomagnetic latitude Φ_N and MLT t_W of the asterisks (symbols Φ_N and t_W were introduced in section 2). Note that after the first substorm onset at 0919 UT the value of t_W varied by a small jump from ~2315 MLT to ~2115 MLT during a few minutes; this was followed by a plateau (see Figure 4). After 0937 UT a larger jump of t_W was observed to reach a value of ~1600 MLT, assuming that large scale current wedge was produced in the interval 0937-0940 UT.

Let us now consider Figure 3b, which shows the distribution of FAC density. Closed dotted contours denote the uncorrected polar cap boundaries for each time. No correction (to be explained below) was introduced in order to give the reader a more pictorial rendition of the method of determining the polar cap boundary. One can see that at 0915 UT (when a clear *DP* 2 type was observed) the three FAC regions of *Iijima and Potemra* [1976] are readily identified in the distribution of FAC density. Indeed, the near-pole region shows upward FAC in the morning sector and downward FAC in the evening sector, which corresponds to FAC region 3; downward FAC in the morning sector and upward FAC in the evening sector are observed at a lower latitude, which corresponds to FAC region 1; and at a still lower latitude one again observes upward FAC in the morning sector and downward FAC in the evening sector, i.e., FAC region 2.

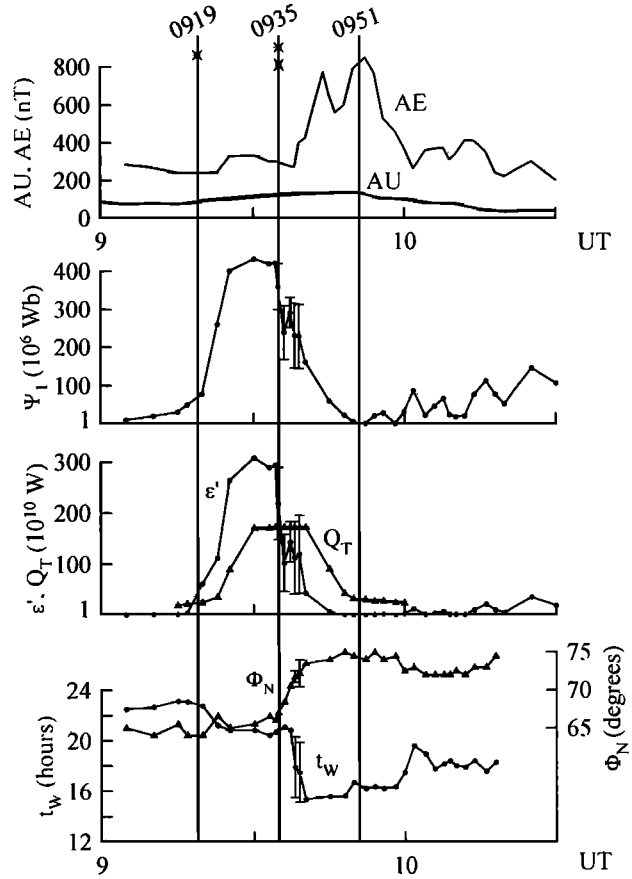

Figure 4. Plots of *AE*, *AU*, and MIT outputs for the CDAW 9C substorm: open tail magnetic flux (Ψ_1), Poynting flux input into the magnetosphere (ε'), total substorm power (Q_T), and coordinates (t_W and Φ_N) of the western end of the westward electrojet. The single asterisk marks the start of the first active phase. The double asterisk denotes expansion onset.

The three FAC regions are extended in latitude when compared with those in the familiar scheme by Iijima and Potemra, which (an extension) leads to a decrease in the polar cap area. This extension is caused by truncation of the series of Legendre polynomials, approximating the magnetic potential of the geomagnetic variation field. The decrease in PC area depends on the length of the polynomial series used. In the cases under consideration, the polynomial series $P_n^m(\cos\theta)$ was used, where n=1–26 and m=0–4. According to specially performed numerical simulations, for the aforementioned polynomial series the truncation effect is compensated within ~10% by multiplying the PC area by the correction factor $\eta = 2.0$ (see *Mishin*, [1990, pp. 91, 156-157] for details). This correction factor is taken into account in plots of Ψ and ε' values in Figure 4 of the present work, although it is not shown in Figure 3.

It is easy to see that the truncation effect creates also an underestimate of U_{PC} values by a factor of $\sqrt{\eta} = \sqrt{2}$.

Let us return to Figure 3b, 0915 UT. Despite the aforementioned truncation effect, the three FAC regions from the scheme by Iijima and Potemra are relatively readily identified in this case, thus permitting us to determine the polar cap boundary shown by the dotted line (the high-latitude boundary of FAC region 1). It is less easy to identify the boundary of FAC region 1 at 0935 UT when the $DP\ 2 \Rightarrow DP\ 1$ transition was in progress. At this instant some details appear inside of the supposed polar cap which do not correspond to the aforementioned classical scheme. At this point and there after we use, as additional information, the equivalent current system (Figure 3a, 0935 UT), enabling us to determine the low-latitude boundary of FAC region 1 by identifying this boundary with the central line of the auroral electrojet. With such an approach, despite the aforementioned uncertainty, it is apparent from the figure that in the interval 0915-0935 UT the polar cap area was growing. Note that the downward FAC region, denoted by the symbol "Y" in Figure 3b, is located inside of the polar cap at 0935 UT, when the $DP\ 2 \Rightarrow DP\ 1$ transition still was in the prefinal stage This means that two westward electrojets of the DP 2 system (which were mentioned in a description of Figure 3a above) had not yet merged together.

Let us now consider Figure 3b for 0940 UT, when the $DP\ 2 \Rightarrow DP\ 1$ transition was completed and the two aforementioned electrojets had merged. One can see that downward FAC region 1, which was localized mainly in the morning sector at 0935 UT and earlier, now extended deep into the evening sector and merged together with region Y. As a result, we can conclude that the polar cap area is decreased markedly during the time interval 0935-0940 UT.

The type of equivalent current systems at the interval 0935-0939 UT cannot be identified without ambiguity. Therefore in Figure 3a for 0938 UT (as well as for 0939 UT) two asterisks, rather than one, mark the supposed termination of the westward electrojet, to which correspond two variants of the polar cap boundary in Figure 3b (i.e., with and without region Y inside of the polar cap). Accordingly, use was made of Ψ_1 values for both variants at the interval 0935-0939 UT, and their average values are shown on plot of Ψ_1 in Figure 4. Vertical bars show the difference of Ψ_1 values for the two variants.

The Ψ_1 plot in Figure 4 illustrates the process considered in greater detail.

Figure 4 gives also the plots of activity indices. The indices were obtained using data from 12 stations. From Figure 4 it is apparent that the first substorm onset created a growth of the AU index to 95 nT and of the AE index to 380 nT. The growth of these indices in response to the final stage of the second supposed substorm onset at 0938-0940 UT reached 130 nT and 860 nT, respectively. The same difference of the two substorm onsets is observed on the intensity plots of the two auroral electrojets (the plots are not shown).

The plots of ε' and Q_T presented in the same figure, where a calculation of Q_T was performed with values of τ according to *Gonzalez et al.* [1989]. The value of $\tau = 0.5$ hour was used for the time interval 0925-0940 UT, when the energy input $\varepsilon' \sim 10^{12}$ W occured (Figure 4), which corresponds to the storm main phase rather than a recovery phase. The input power $\varepsilon' \leq 1 \times 10^{11}$ W and declining values of D_{st} - index are seen in Figure 6 at 0900-0919 and 0945 UT, both of which are the signatures of the storm recovery phase Therefore we used the value of $\tau = 7.0$ hour for these two time intervals, and an intermediate value of τ for the intervals 0920-0925, and 0940-0945 UT. As a result, it is seen in Figure 4 that the difference $P = \varepsilon' - Q_T$ was positive, i.e., the external energy source ensured the total observed disturbance power; thus it was mainly a driven disturbance in the interval 0919-0935 UT. After the second onset the difference $\varepsilon' - Q_T$ decreases rapidly and becomes negative. In this case, $\varepsilon' \Rightarrow 0$ while $AE \Rightarrow max$. Obviously, the disturbance energy after the second onset is ensured mainly by the intramagnetospheric source; the disturbance becomes mainly unloading.

An important additional information about the spatial localization of the two onsets is contained in Figure 5, showing 11 available X magnetograms from stations that recorded at least one of the onsets with a selected (crude, see the figure) sensitivity. The figure shows the station's latitude and MLT at 0919 UT, which permits a rough evaluation of the visibility region size for each onset.

One can see that the visibility zone was limited by a low-latitude boundary $\Phi \approx 60°$ (Sitka) for both onsets. The high-latitude boundary of this zone is $\Phi \approx 65°$ (College) for the first onset and $\Phi \approx 71°$ (Inuvik) for the second onset. A disturbance maximum was observed near $\Phi \approx 65°$ at the time of occurrence of both onsets. Thus the instability that produced the second onset occurred on the highlatitude boundary of the first onset source region; this region expanded tailward in the course of the second onset. Similarly, ground-based magnetometers "saw" the first onset in a narrow longitudinal sector (2200-2300 MLT) and the second onset in a wider longitudinal sector (2100-0100 MLT). The transition from the first to the second onset was not a continuous process but rather was a discrete process. The second onset started after the first when this substorm intensification had partly decayed. This start (of the second onset) took place in another domain of the plasma sheet and involved a new sort of physics: the open tail reconnection.

Figure 5 shows quite clearly the localized substorm onset at Fort Yukon, which was observed a little earlier than 0935 UT. Figure 5 shows also clearly the 0936 UT onset at College. Therefore we cannot accept 0938 UT as the second substorm onset start time if the latter is defined as the earliest from observed. There are two additional arguments supporting the view that the earliest onset at ~0935 UT was not too spatially localized.

1. Hones et al. (unpublished manuscript, 1993) noted

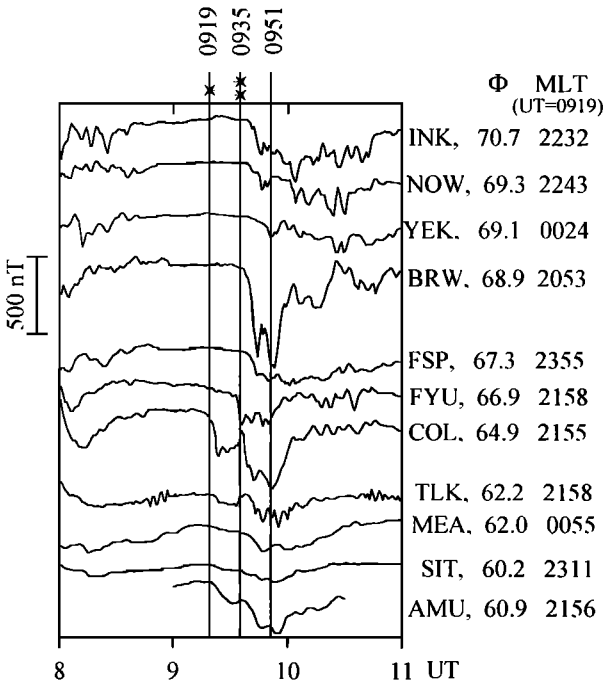

Figure 5. X component magnetograms from some magnetometer stations: Inuvik (INK), Norman Wells (NOW), Yellowknife (YEK), Barrow (BRW), Fort Simpson (FSP), Fort Yukon (FYU), College (COL), Talkeetna (TLK), Meanook (MEA), Sitka (SIT), and Anchorage (AMU). Magnetic latitudes and local times are indicated. The single asterisk marks the start of the first active phase. The double asterisk denotes expansion onset.

0936 UT as the substorm onset, using both the College magnetogram and data from satellite 1984-129 (see section 3).

2. Plots of Ψ_1 and ε' (Figure 4) (as well as a comparison of the polar cap areas in Figure 3b for 0935 and 0938 UT) indicate that the rapid decrease of these parameters began just after 0935 UT.

As the resume, we determine the whole interval 0935-0940 UT as the time of the second substorm onset. The principal signature of this onset is a rapid decrease of the open tail magnetic flux Ψ_1, the start of which was observed at ~0935 UT (Figure 4). Earliest, spatially localized signatures of the onset were also observed at ~0933, 0936, and 0936 UT, respectively, on magnetograms of Fort Yukon, and College, and data of synchronous satellite 1984-129. Subsequent, global signatures were observed at 0938-0940 UT in the form of a sudden accelerated transformation of the equivalent current system from *DP* 2 to *DP* 1 type (Figures 4 and 3a), and a corresponding change of the FAC system (Figure 3b), and in the form of rapidly increasing *AE* indices (Figure 4).

Now we can try to express the conclusions obtained on two successive substorm onsets in terms of phases of a typical substorm. *Mishin* [1991] and *Mishin et al.* [1992a] argued that in a typical substorm there are two sorts of substorm onsets with two kinds of physics which are related to two subsequent active phases of a typical substorm. They described typical observed signatures of each phase and called them, respectively, the first and second (expansion) phase. In this connection, all the foregoing with regard to the intervals 0919-0935 and 0935-0950 UT enables us to relate these two intervals to the first active and expansive phase, respectively. A first active phase is, primarily, a driven process, a second (expansion) phase is mainly an unloading process. These conclusions and different physics of two active phases will be discussed additionally in the next section.

Thus we identified two active phases of the substorm considered, but not the growth and recovery phases. The latter was identified and described by Hones et. al. with its start at 0951 UT (section 3). MIT data support this conclusion (see Figure 4) without adding anything essentially new on the recovery phase. A more interesting task is to identify the prephase, i.e., growth phase of the substorm considered, which is expected to be a driven process, when input power ε' and activity index AE are both correlated positively with the dayside magnetopause reconnection rate M.

Figure 6 contains some information about the prehistory of the event being studied, i.e., the plots of U_{PC}, t_W, D_{st}, and ε' for the interval 0600-1100 UT. U_{PC} is the polar cap potential drop calculated by MIT as the difference between maximum and minimum values of the electric potential in the ionosphere of the dayside polar cap [*Mishin*, 1991]. U_{PC} values in Figure 6 corrected by multiplying by $\sqrt{2}$ (see above "the series of Legendre polynomials truncation effect"). It is known that U_{PC} can be considered to be the result of a transfer in the ionosphere of the solar wind potential drop M on the dayside magnetopause reconnection line [e.g., *Lockwood* 1991]. Therefore it is possible to use the plot of U_{PC} in Figure 6 as a tentative substitute of M plot for the time interval 0830-0935 UT. This interval does not include the expansion phase but covers the loading phase of the substorm considered, because a growth of the input power ε' (and hence the open tail magnetic flux Ψ) is observed through this interval. Using in addition the Figure 3 data, one can see that the positive difference $\varepsilon' - Q_T$ occurs at 0910-0935 UT. The total energy loaded during this latter interval is close to 1×10^{22} erg. However, returning to Figure 6, one may note that there is no expected positive correlation between U_{PC} and input power ε' during and before the load. It means (in terms of the model where U_{PC} is the substitute for M) that the substorm under consideration was not stimulated by an increasing of M during its loading phase. Hence (in terms of the same model) it was a special type substorm, with the loading phase stimulated by intramagnetosphere processes The physics of this special loading process will be discussed in the next section.

A substorm growth phase is usually defined as a time interval with signatures of storage of the magnetotail energy but without substorm onsets. Such signatures are observed in the interval 0910-0919 UT. Thus we

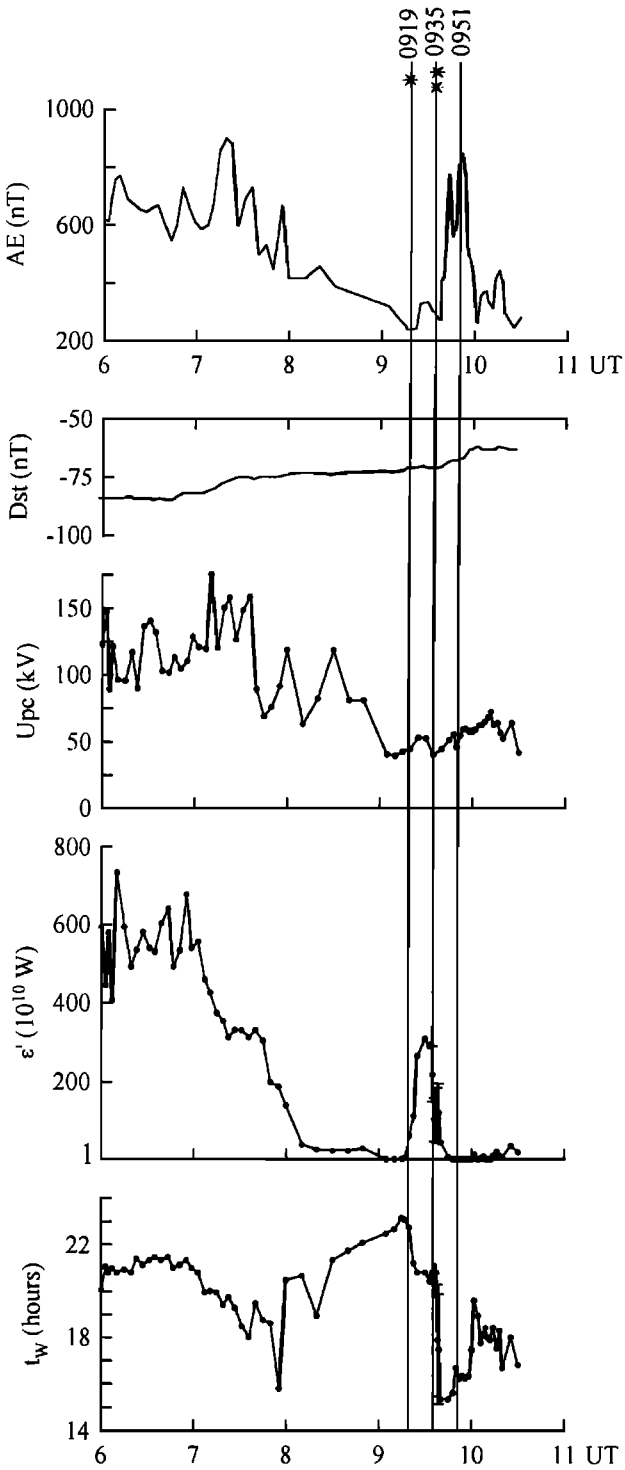

Figure 6. Plots of AE, D_{st}, and MIT 2 outputs for the interval 0600-1030 UT, May 3, 1986: polar cap potential (U_{PC}), Poynting flux input into the magnetosphere (ε'), and MLT of the western termination of the westward electrojet (t_W). The single asterisk marks the start of the first active phase. The double asterisk denotes expansion onset.

will call this interval the growth phase, although it was a special growth phase, i.e., without growth of U_{PC}.

We have identified the following phases in the substorm: the first active phase during 0919-0935 UT, the expansion phase at 0935-0951 UT, and the recovery phase at 0951-1030 UT, as well as (though less clearly) a short-lasting growth phase at 0910-0919 UT. Starts of phases at 0919 and 0951 UT are both determined according to Hones et al., which does not contradict the MIT data in Figure 4. However, the expansion onset at 0933-0935 UT, determined from MIT data, differs from the moment in time 0936 UT which was determined by Hones et al. using synchronous orbit data. The expansion onset in MIT (i.e., ground) data is ahead of that in geostationary orbit by 1 to 3 min. *Sauvaud* [1992] estimated the velocity of the injection front earthward propagation to be between 64 and 140 km/s. Using 100 km/s and a delay of 1.5 min, we will find, for the initial location of the current reduction, a radial distance of 8.1 R_E following *Sauvaud* [1992]. With 140 km/s and a delay of 3 min we have for the same distance about 11 R_E. Thus this initial distance of the open tail reconnection region is from 8 to 11 R_E, which is markedly tailward of the region of 0919 UT onset. Subsequently, the open tail reconnection (the expansion onset) region propagates still farther tailward.

5. Discussion and Conclusions

An analysis of the substorm of May 3, 1986, 0910-1030 UT has been made in this paper by using the data base reported by *Hones et al.* [1987, also unpublished manuscript, 1993] and additional MIT 2 data. We have identified the signatures of classical growth, expansion, and recovery phases in the intervals 0910-0919, 0935-0950 and 0951-1030 UT, respectively. However, the interval 0919-0935 UT could not be identified unambiguously from the Hones et al. data. Additional MIT 2 data have demonstrated that this interval does not correspond to the expected signatures of any one of the above phases:

1. In the beginning of the interval 0919-0935 UT a clear substorm onset occurred, but its signatures were observed in a narrow sector, ~2200-2300 MLT at latitudes $\Phi \leq 65°$, which is mapped to the innermost current sheet where no large-scale neutral line has ever been observed.

2. A current system, approaching the *DP* 2 type, (i.e., corresponding to a directly driven mechanism, which is fed by an external energy source) was observed in the interval 0919-0935 UT, which confirms the absence of large-scale cross-tail current disruption. The sign of the difference $\varepsilon' - Q_T$ was positive at 0919-0935 UT, which also means predominance of the external disturbance energy source (in contrast to the interval 0935-0950 UT).

3. The open tail magnetic flux was increasing in the interval 0919-0935 UT, which excludes open tail reconnection as the predominating trend in this interval.

The aforementioned signatures in 0919-0935 UT are consistent with those for a special substorm phase containing so-called "multiple onsets" and said to be the "first active phase" [*Mishin et al.*, 1992a, and references therein]. Obviously, this phase differs from the

expansion phase. This phase differs also from the growth phase by a higher activity level, the presence of substorm onsets observed on the ground and near geosynchronous orbits, and the presence of corresponding small-scale current disruptions. Accordingly, the phase of multiple onsets is characterized by a special physics: instabilities in the innermost current sheet, not peculiar to the early growth phase, i.e., to the "simple" loading process which is observed prior to substorm onsets.

In the aforementioned general scenario, a "special physics" of the first active phase involves (in addition to the aforementioned instabilities) still another supposed peculiarity. This is a chain of processes created by the tail stretching with a positive feedback (TSF for short). The hypothesis of TSF offers a clearer explanation of why substorms (in the scope of the scenario) follow the same scheme of development: growth phase - multiple onsets - expansion - recovery phase. TSF assumes a continuous growth of the input power ε' after an initial jump of dayside magnetopause reconnection rate M, even if M are maintained after the jump on the constant initial level. Indeed, as a consequence of the initial growth of input energy ε', the intensity J_T of cross-tail current would increase, and, as a consequence, the tail length l_T would also increase. From formula (13) (section 2) it follows that the growth of the tail length leads to a further increase of input energy ε' (even when M=const), and so on, continuously, with the positive feedback, until a threshold of a special instability would be attained, which can stop TSF and create a collapse of the tail.

Growth of J_T and l_T, in itself, means a growth phase A continuation of this process leads to first instabilities in the innermost (and most intense) current sheet and, accordingly, to the first active phase, which, however, cannot stop TSF. As this phase progresses, a growth of ε', J_T and l_T continues, thus creating the next instability, which is observed tailward of the first one. This second (in time) instability is observed to include the open tail reconnection, which creates the expansion onset, although it stops the development of TSF. If the external conditions that have generated TSF persist for a long time, then the tail length recovers during the recovery phase or a little later, and the cycle of three (without growth phase) or four standard phases is expected to recur, even with a stationary solar wind (at a sufficiently high level of M and ε).

This hypothesis is the result of studying a number of substorms using a conventional data base including the solar wind data, and, in addition, data of MIT 2. Unfortunately, it is impossible to test the hypothesis of TSF with a conclusive result in this study, because the solar wind data were unavailable. Nevertheless, one new supporting argument may be mentioned using the polar cap potential drop U_{PC} as the tentative substitute of dayside magnetopause reconnection rate M. With such an approach, we can explain the special character of the substorm growth phase mentioned in section 4, i.e., lack of a positive correlation between ε' and Ψ_1, on the one hand, and U_{PC}, on the other, which was observed at the interval 0830-0935 UT when input power ε' was growing an order of magnitude (Figure 6). Indeed, growth of Ψ_1 and ε', observed when U_{PC} is decreased or remains unchanged, can be interpreted using formulas (12) and (13), as the result of strong tail stretching, due to TSF, in the course of this interval.

At this point, we return to the question of the nature of instabilities in the innermost current sheet. Earlier, we pointed out that multiple onsets seem to be initiated by some instability that diverts the innermost, very intense, part of the tail current sheet into a current wedge via the auroral ionosphere [*McPherron*, 1989]. The power comes mostly from the solar wind but also from magnetic energy in the immediate vicinity of the wedge due to partial tail collapse in a limited local time sector. The nature of the instability is still a matter of speculation. Different models have been proposed. One possibility is electron chaotization that leads to a tearing mode instability [*Buchner and Zelenyi*, 1987; *Pulkkinen et al.*, 1991]. Other possibilities are a sudden appearance of double layers above the brightening auroral arc through a feedback instability in the ionosphere-magnetosphere current circuit as in the RBSF model [*Block et al.*, 1986; *Rothwell et al.*, 1988b, 1991], current disruption of the intense dawn-dusk current at the inner edge of the plasma sheet [Lui, 1991], a thermal catastrophe [*Goertz and Smith*, 1989], or a Rayleigh-Taylor-like instability at the inner edge of the plasma sheet [*Roux et al.*, 1991].

Thus the nature of instabilities in the innermost current sheet is not completely clear, but relatively low thresholds for these instabilities (in terms of J_T, l_T, and ε') and spatial region with closed field lines distinguishes them from those of unloading process, which predominates during expansion onset. Therefore we assume that two active phase have different physics. Such an assumption is consistent with the synthesis model of *Lui* [1991] where the active substorm period is also divided into two different stages which are similar to our two active phases.

Now, we will discuss the second active (expansion) phase. Unloading processes seem to be triggered often by a sudden decrease in power input from the solar wind, much in the same manner as a sudden switching off of the generator in an inductive circuit, when previously loaded energy immediately induces high voltage at the switch (above the brightening arc) where a large fraction of the energy is dissipated. In the case discussed above, however, IMF data were unavailable Using the plot of U_{PC} as an indirect indicator of a power input from the solar wind, one can see (Figure 6) that the expected signature of the triggered expansion onset was not observed in the event considered. It seems likely that the expansion onset was a spontaneous one. If this is true, then a fast decrease of ε', observed in the interval of 0935-0940 UT (Figure 4), is not the cause but a consequence of the process that produced the expansion onset.

One more remark about some of substorm models

is in order. The results in section 4 appear to contradict the neutral line model, which is hard to reconcile with the large expansion of the westward electrojet all the way to 1600 MLT. The M-I coupling model of *Kan* [1991] predicts large northwestward expansion of the aurora and the westward electrojet (as observed after expansion onset), but only as an externally (solar wind) driven process. However, our analysis shows that expansion onsets are usually powered internally within the magnetosphere, since the energy input ε' from the solar wind does not cover the dissipation within the magnetosphere-ionosphere system.

There is, on the other hand, no apparent conflict between our results and the M-I coupling model of *Rothwell et al.* [1989] and of *Lui* [1991].

On the whole, this case study of a CDAW 9C substorm supports the scenario with two active phases, although the unavailability of solar wind parameters has limited considerably the potential of our analysis.

6. Summary

The MIT 2 technique, described in section 2, ensures the determination of the polar cap boundaries and area and hence of both the variable magnetic flux in the "open" tail (Ψ_1) and the always persisting "quasi-open" magnetic flux in the near-pole part of the polar cap (Ψ_2). The plot of Ψ_1 visualises the dynamics of the dayside magnetic merging and nightside reconnection in the course of the event considered. With a knowledge of Ψ_1 and the solar wind parameters V and IMF, it is possible to calculate the energy input to the magnetosphere (ε'), the efficiency of the solar wind - magnetosphere dynamo, and the variable tail length. The fact that values of $\Psi_2 \geq 3 \times 10^8$ Wb are observed all the time leads to a model of the geomagnetosphere involving, along with the open tail, also a quasi-open tail, whose field lines intersect the equatorial plane but are of such a length that they lose the properties of a magnetic trap.

MIT 2 data that were used as additional information, made it possible to reveal new features of the substorm of May 3, 1986, 0900-1030 UT, as described earlier by *Hones et al.* [1987, also unpublished manuscript, 1993]. The main features characterize the differences of processes which produced two substorm onsets, at 0919 and ~0935 UT.

1. It has been pointed out that the open magnetic flux Ψ_1 continues to grow following the first substorm onset and that Ψ_1 decreases rapidly just after (or around) the second onset.

2. The ionospheric current system kept the type similar *DP* 2 after the first onset but changed rapidly to the *DP* 1 type after the second onset.

3. The disturbed region was localized at $x < 8R_E$ after 0919 UT but propagated rapidly tailward after the second onset at 0935 UT (this latter was also pointed by Hones et al.).

4. The difference $\varepsilon' - Q_T$ remained positive after 0919 UT (which indicates the predominance of an external disturbance energy source) but changed sign shortly after ~ 0935 UT.

5. Both onsets, like the substorm as a whole, were following a marked decrease of values of U_{PC}, although it kept its high value, similarly to the input power and the ring current intensity. Therefore, and using U_{PC} as an substitute of the dayside magnetopause reconnection rate M, we suppose that the substorm considered belongs to those arising spontaneously, without increasing of M.

On the whole, based on the extended data set it has been possible to describe the event considered of May 3, 1986, in the frames of the substorm scenario with two active phases. Its characteristic property, compared with the conventional scenario, is the phase of multiple onsets, also called the "first active phase." This phase is created by instabilities in the innermost current sheet, without neutral line formation.

Acknowledgments. V. Mishin thanks The Royal Swedish Academy of Sciences, Bengt Hultqvist at the Swedish Institute of Space Physics, and C.-G. Falthammar at the Royal Institute of Technology for financial support and hospitality during a four-month visit to Sweden, when much of this work was carried out. Partial funding was provided by Russian Fund for Fundamental Research Grants NN 9302117017 and 960564348, and Soros Foundation Grants NN U19000 and U19300.

The Editor thanks Ioannis A. Daglis and another referee for their assistance in evaluating this paper.

References

Akasofu, S.-I., *Polar and Magnetospheric Substorms*, 354 pp., D. Reidel, Norwell, Mass., 1968.

Akasofu, S.-I., *Physics of Magnetospheric Substorms*, 599 pp., D. Reidel, Norwell, Mass., 1977.

Akasofu, S.-I., Energy coupling between the solar wind and the magnetosphere, *Space Sci. Rev., 28*, 121-190, 1981.

Akasofu, S.-I., A new era in magnetospheric research, in *Substorm 1. Proceedings of the First International Conference on Substorm, Eur. Space Agency Spec. Publ., ESA SP-335*, 5-9, 1992.

Akasofu, S.-I., C.-I. Meng, and K. Makita, Changes of the size of the open field line region during substorms, *Planet. Space Sci., 40*, 1513-1524, 1992.

Baker, D. N., Driven and unloading aspects of magnetospheric substorms, in *Substorm 1, Proceedings of the First International Conference on Substorm, Eur. Space Agency Spec. Publ., ESA SP-335*, 185-191, 1992.

Baker, D. N., T. I. Pulkkinen, R. L. McPherron, and C. R. Clauer, Multi spacecraft study of a substorm growth and expansion phase features using a time-evolving field model, in *Solar System Plasmas in Space and Time, Geophys. Monogr. Ser.*, vol. 84, edited by J. L. Burch and J. H. Waite Jr., pp. 101-110, AGU, Washington, D.C., 1994.

Birn, J., E. W. Hones Jr., J. D. Craven, L. A. Frank, R. D. Elphinstone, and D. P. Stern, On open and closed field line regions in Tsyganenko's field model and their possible associations with horse collar auroras. *J. Geophys. Res., 96*, 3811-3817, 1991.

Block, L. P., P. L. Rothwell, and M. B. Silevitch, A new model for substorm breakup (abstract), *Eos Trans. AGU, 67*, 1178-1179, 1986.

Buchner, J., and L. M. Zelenyi, Chaotization of the electron motion as the cause of an internal magnetotail instability

and substorm onset, *J. Geophys. Res., 92,* 13,456-13,466, 1987.

Coroniti, F., R. L. McPherron, and G. K. Parks, Studies of the magnetospheric substorm, 3, Concept of the magnetospheric substorm and its relation to electron precipitation and micropulsations, *J. Geophys. Res., 73,* 1715-1722, 1968.

Elphinstone, R. D., K. Jankowska, J. S. Murphree, L. L. Cogger, D. Hearn and G. Marklund, The configuration of the auroral distribution for interplanetary magnetic field B_Z northward, 1, IMF B_X and B_Y dependencies as observed by the Viking satellite, *J. Geophys. Res., 95,* 5791-5804, 1990.

Elphinstone, R. D., D. Hearn, J. S. Murphree, and L. L. Cogger, Mapping using the Tsyganenko long magnetospheric model and its relationship to Viking auroral images, *J. Geophys. Res., 96,* 1467-1480, 1991.

Goertz, C. K., and R. A. Smith, Thermal catastrophe model of substorms, *J. Geophys. Res., 94,* 6581-6596, 1989.

Gonzalez, W. D., B. T. Tsurutani, A. L. C. Gonzalez, E. J. Smith, F. Tang, and S.-I. Akasofu, Solar wind - magnetosphere coupling during intense magnetic storms, *J. Geophys. Res., 94,* 8835-8851, 1989.

Hill, T. W., Solar wind - magnetosphere coupling, in *Solar-Terrestial Physics,* edited by R. L. Carovillano and J. M. Forbes, pp. 261-302, D. Reidel, Norwell, Mass., 1983.

Hones, E. W., Jr., C. D. Anger, J. Birn, J. S. Murphree, and L. L. Cogger, A study of a magnetospheric substorm recorded by the Viking auroral imager, *Geophys. Res. Lett., 14,* 411-414, 1987.

Iijima, T., and T. A. Potemra, Field-aligned currents in the dayside cusp observed by TRIAD, *J. Geophys. Res., 81,* 5971-5979, 1976

Jankowska, K., R. D. Elphinstone, J. S. Murphree, L. L. Cogger, D. Hearn, and G. Marklund, The configuration of the auroral distribution for interplanetary magnetic field B_Z northward, 2, Ionospheric convection consistent with Viking observations, *J. Geophys. Res., 95,* 5805-5816, 1990.

Kamide, Y., A. D. Richmond, and S. Matsushita, Estimation of ionospheric electric fields, ionospheric currents, and field-aligned currents from ground magnetic records, *J. Geophys. Res., 86,* 801-813, 1981.

Kan, J. R., Dipolarization: A consequence of substorm expansion onset, *Geophys. Res. Lett., 18,* 57-60, 1991.

Kan, J. R., A global magnetosphere-ionosphere coupling model of substorms, *J. Geophys. Res., 98,* 17,263-17,275, 1993.

Kan, J. R., and L. C. Lee, Energy coupling function and solar wind-magnetosphere dynamo, *Geophys. Res. Lett., 6,* 577-580, 1979.

Lockwood, M., The exitation of ionospheric convection, *J. Atmos. and Terr. Phys., 53,* 177-199, 1991.

Lui, A. T. Y., A synthesis of magnetospheric substorm models, *J. Geophys. Res., 96,* 1849-1856, 1991.

Lyons, L. R., A new theory for magnetospheric substorms, *J. Geophys. Res., 100,* 19,069-19,081, 1995.

Lyons, L. R., Substorms: Fundamental observational features, distinction from other disturbances, and external triggering, *J. Geophys. Res., 101,* 13,011-13,025, 1996.

Marklund, G. T., L. G. Blomberg, T. A. Potemra, J. S. Murphree, F. J. Rich, and K. Stasiewicz, A new method to derive "instantaneous" high-latitude potential distributions from satellite measurements including auroral imager data, *Geophys. Res. Lett., 14,* 439-442, 1987.

McPherron, R. L., Growth phase of magnetospheric substorms, *J. Geophys. Res., 75,* 5592-5599, 1970.

McPherron, R. L., Studies of geomagnetic activity using operational geostationary satellites (abstract), *Eos Trans. AGU, 70*(15), 438, 1989.

McPherron, R. L., C. T. Russell, and M. P. Aubry, Satellite studies of magnetospheric substorms on August 15, 1968, 9, Phenomenological model for substorms, *J. Geophys. Res., 78,* 3131-3149, 1973.

Mishin, V. M., On the electric currents in the magnetosphere (in Russian), *Geomagn. Aeron., 8,* 168-171, 1968.

Mishin, V. M., The magnetogram inversion technique and some applications, *Space Sci. Rev., 53,* 83-163, 1990.

Mishin, V. M., The magnetogram inversion technique: Applications to the problem of magnetospheric substorms, *Space Sci. Rev., 57,* 237-337, 1991.

Mishin, V. M., A. D. Bazarzhapov, and G. B. Shpynev, Electric fields and currents in the Earth's magnetosphere, in *Dynamics of the Magnetosphere, Astrophys. Space Sci. Libr.,* vol. 78, edited by S.-I. Akasofu, pp. 249-268, D. Reidel, Norwell, Mass., 1979.

Mishin, V. M ., S. B. Lunyushkin, D. Sh. Shirapov, and W. Baumjohann, A new method for generating instantaneous ionospheric conductivity models using groundbased magnetic data, *Planet. Space Sci., 34,* 713-722, 1986.

Mishin, V. M., T. I. Saifudinova, A. D. Bazarzhapov, D. Sh. Shirapov, and S. B. Lunyushkin, The magnetospheric substorm scenario "with two active phases", in *Substorm 1, Proceedings of the First International Conference on Substorm, Eur. Space Agency Spec. Publ., ESA SP-335,* 297-302, 1992a.

Mishin, V. M., J. Woch, L. Eliasson, T. I. Saifudinova, A. D. Bazarzhapov, D. Sh. Shirapov, and S B. Lunyushkin, Substorm scenario with two active phases: A study of CDAW-9C events, in *Substorm 1, Proceedings of the First International Conference on Substorm, Eur. Space Agency Spec. Publ., ESA SP-335,* 383-388, 1992b.

Perreault, P., and S.-I. Akasofu, A study of geomagnetic storms, *Geophys. J. R. Astron. Soc., 54,* 547-573, 1978.

Piddington, J. H., Theories of the geomagnetic storm main phase, *Planet. Space Sci., 11,* 1277-1288, 1963.

Pulkkinen, T. I., D. N. Baker, D. N. Fairfield, R. J. Pellinen, J. S. Murphree, R. D. Elphinstone, R. L. McPherron, J. F. Fennel, R. E. Lopez, and T. Nagai, Modeling the growth phase of substorm using the Tsyganenko model and multispacecraft observations: CDAW-9, *Geophys. Res. Lett., 18,* 1963-1966, 1991.

Richmond, A. D., and Y. Kamide, Mapping electrodynamic features of the high-latitude ionosphere from localized observations: Technique, *J. Geophys. Res., 93,* 5741-5759, 1988.

Rothwell, P. L., M. B. Silevitch, L. P. Block, and P. Tanskanen, A model of the westward traveling surge and generation of Pi 2 pulsations, *J. Geophys. Res., 93,* 8613-8624, **1988a.**

Rothwell, P. L., L. P. Block, M. B. Silevitch, and C.-G. Falthammar, A new model for substorms onsets: The prebreakup and triggering regimes, *Geophys. Res., Lett., 15,* 1279-1282, **1988b.**

Rothwell, P. L., L. P. Block, M. B. Silevitch, and C.-G. Falthammar, A new model for auroral breakup during substorms, *IEEE Trans. Plasma Sci., 17,* 150-157, 1989

Rothwell, P. L., M. B. Silevitch, L. P. Block, and C.-G. Falthammar, Prebreakup arcs: A comparison between theory and experiment, *J. Geophys. Res., 96,* 13,967-13,975, 1991.

Roux, A., S. Perreault, P. Robert, A. Morane, A. Pedersen, A. Korth, G. Kremser, B. Aparicio, D. Rodgers, and R. Pellinen, Plasma sheet instability related to the westward traveling surge, *J. Geophys. Res., 96,* 17,697-17,714, 1991.

Russell, C. T., The control of the magnetopause by the interplanetary magnetic field, in *Dynamics of the Magnetosphere, Astrophys. Space Sci. Libr.*, vol. 78, edited by S.-I. Akasofu, pp. 3-21, D. Reidel, Norwell, Mass., 1979.

Sauvaud, J.-A., Characteristics of the cross-tail current disruption at substorm onset and associated particle acceleration, in *Substorm 1, Proceedings of the First International Conference on Substorm, Eur. Space Agency Spec. Publ., ESA SP-335*, 243-253, 1992.

Siscoe, G. L., and W. D. Cummings, On the cause of geomagnetic bays, *Planet. Space Sci., 17*, 1795-1802, 1969.

Zwickl, R. D., L. F. Bargatze, D. N. Baker, C. R. Clauer, and R. L. McPherron, An evaluation of the total magnetospheric energy output parameter, U_T, in *Magnetotail Physics*, edited by A.T.Y.Lui, pp. 155-159, Johns Hopkins Univ. Press, Baltimore, Md., 1987.

A. D. Bazarzhapov, S. B. Lunyushkin, V. M. Mishin, and T. I. Saifudinova, Institute of Solar-Terrestrial Physics, Russian Academy of Sciences, P.O.Box 4026, Irkutsk, 664033, Russia. (e-mail: root@sitmis.irkutsk.su)

L. P. Block, L. G. Blomberg, and G. T. Marklund, Alfven Laboratory, Department of Plasma Physics, Royal Institute of Technology, S-10044 Stockholm, Sweden. (e-mail: block@plasma.kth.se)

L. Eliasson, Swedish Institute of Space Physics, P.O.Box 812, S-98128 Kiruna, Sweden. (e-mail: lars@irf.se)

H. Opgenoorth, Swedish Institute of Space Physics, S-75591 Uppsala, Sweden. (e-mail: opg@irfu.se)

D. Sh. Shirapov, East Siberian State Technology University, Ulan-Ude, Russia

J. Woch, Max-Planck-Institut für Aeronomie, Postfach 20, D-37189 Katlenburg-Lindau, Germany (e-mail woch@linmpi.dnet.gwdg.de)

(Received April 23, 1992; revised December 3, 1996, accepted January 10, 1997.)